Diffraction of a Plane Skew Electromagnetic Wave by a Wedge With General Anisotropic Impedance Boundary Conditions

Bair V. Budaev and David B. Bogy

***Abstract*—The three dimensional problem of diffraction of a skew incident plane wave by a wedge with anisotropic impedance boundary conditions is explicitly solved by the probabilistic random walk method. The problem is formulated in terms of two certain components of the electric and magnetic fields which satisfy independent Helmholtz equations but are coupled through the first-order boundary conditions. The solution is represented as a superposition of the geometric waves that are completely determined by elementary methods and of the waves diffracted by the apex of the wedge. The diffracted field is explicitly represented as the mathematical expectation computed over the trajectories of a two-state random motion which runs in a complex space and switches states under the control of stochastic equations determined by the problem's geometry and by the boundary conditions.**

I. Introduction

In the last decade there has been an increasing interest in studying the diffraction of electromagnetic waves by an infinite wedge with impedance boundary conditions [2], [20], [25], [26]. If the surface impedances are isotropic and the incident wave propagates in a direction orthogonal to the wedge's apex, then the problem can be easily split into two scalar problems which can be solved by the Sommerfeld–Maliuzhinets method [19] developed in 1950s. Similar splitting is also possible in some more general cases [2], [18], [21], but it appears that the fundamental problem of diffraction of a skew incident wave by a wedge with general anisotropic impedance boundary conditions does not have a conventional closed-form solution represented by arithmetic operations and quadratures applied to admissible special functions as found in a source such as [1], [27], for example. The latter statement, however, does not eliminate the possibility that there may be other closed-form descriptions of the diffracted waves, such as the probabilistic solutions introduced in [3]–[7] for the analysis of wave propagation.

Here we extend the method from [7] for two dimensional problems of diffraction by an impedance wedge to a general three dimensional problem of electromagnetic diffraction of a skew incident plane wave by a wedge with general anisotropic impedance boundary conditions on its faces. In the formulation we follow [18] where the problem is reduced to a system of two independent Helmholtz equations accompanied by a system of coupled boundary conditions. Then, we employ a decomposition, commonly used in the method of parabolic equations [33], of the unknown wave fields into the predefined geometric component and the diffracted fields which have to be determined. Finally, after a brief introduction in Section IV of the Feynman–Kac probabilistic formulas, we obtain an explicit solution of the considered problem of diffraction.

Manuscript received September 20, 2004; revised October 7, 2005. This work was supported in part by NSF Grants CMS-0098418, CMS-0408381 and in part by the DARPA/AFOSR contract FA 9550-0501-0111. The work of D. Bogy was supported by the William S. Floyd, Jr. Distinguished Professorship in Engineering.

The authors are with the Department of Mechanical Engineering, University of California, Berkeley, CA 94720 USA (e-mail: budaev@berkeley.edu; dbogy@cml.me.berkeley.edu).

Digital Object Identifier 10.1109/TAP.2006.874317

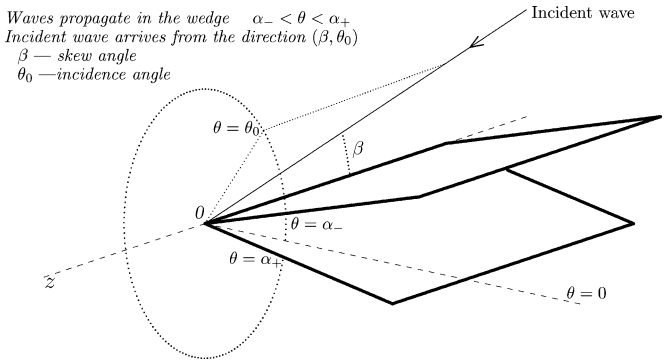

Fig. 1. Geometry of the problem.

II. Formulation of the Problem

Let (r, θ, z) be cylindrical coordinates so that

$$G = \{r, \theta, z: \quad r > 0, \quad \alpha_- < \theta < \alpha_+, \quad -\infty < z < \infty\} \tag{2.1}$$

is a three dimensional wedge (see Fig. 1) parameterized by the angles $\alpha_\pm$, and let

$$\vec{e} = (\sin\beta, \pi + \theta_0, \cos\beta) \tag{2.2}$$

be a unit vector which ends at the center of the coordinates and starts at the point $(\sin\beta, \theta_0, \cos\beta)$ parameterized by the "skew" angle β and the "incident" angle θ_0.

The goal of this work is to compute the electromagnetic field generated by a monochromatic plane wave arriving along the direction $\vec{e}$ to the wedge G which has anisotropic impedance boundary conditions imposed on its faces $\theta = \alpha_\pm$. We consider monochromatic waves with the time dependence specified by the factor $\mathrm{e}^{-\mathrm{i}\omega t}$ which is suppressed hereafter.

It is well-known that the electromagnetic field in the considered configuration is completely characterized by the z-components E_z and H_z of the electric and magnetic vector fields. In particular, the plane incident wave propagating in the direction

$\vec{e}$ is completely characterized by the fields E_z^0 and H_z^0, which have the structure

$$E_z^0 = p_e \mathrm{e}^{-\mathrm{i}kr\sin\beta\cos(\theta-\theta_0)+\mathrm{i}kz\cos\beta}$$
$$Z_0 H_z^0 = p_h \mathrm{e}^{-\mathrm{i}kr\sin\beta\cos(\theta-\theta_0)+\mathrm{i}kz\cos\beta} \tag{2.3}$$

where k is the wave number, p_e, p_h are constants determining the amplitude and polarization of the considered plane wave, and Z_0 is the intrinsic impedance of the medium.

Assuming that the boundary impedances are constants and that the skew angle β belongs to the interval $0 < \beta < \pi$, it is easy to show that the electromagnetic field generated by the incident wave (2.3) can be characterized by two functions $\Phi_1(r,\theta)$ and $\Phi_2(r,\theta)$ introduced by the expressions

$$\Phi_1(kr\sin\beta,\theta) = Z_0 H_z(r,\theta,z)\mathrm{e}^{-\mathrm{i}kz\cos\beta}$$
$$\Phi_2(kr\sin\beta,\theta) = E_z(r,\theta,z)\mathrm{e}^{-\mathrm{i}kz\cos\beta} \tag{2.4}$$

which imply that Φ_1 and Φ_2 obey normalized Helmholtz equations

$$\nabla^2\Phi_1(r,\theta)+\Phi_1(r,\theta)=0, \quad \nabla^2\Phi_2(r,\theta)+\Phi_2(r,\theta)=0 \tag{2.5}$$

formulated in the plane with polar coordinates (r,θ). Additionally, these functions must satisfy the boundary conditions

$$\pm\mathrm{i}\left(\frac{1}{r}\frac{\partial\Phi_1}{\partial\theta}+\cos\beta\frac{\partial\Phi_2}{\partial r}\right)+A_{11}^{\pm}\Phi_1+A_{12}^{\pm}\Phi_2=0, \quad \theta=\alpha_{\pm} \tag{2.6}$$

$$\pm\mathrm{i}\left(\frac{1}{r}\frac{\partial\Phi_2}{\partial\theta}-\cos\beta\frac{\partial\Phi_1}{\partial r}\right)+A_{21}^{\pm}\Phi_1+A_{22}^{\pm}\Phi_2=0, \quad \theta=\alpha_{\pm} \tag{2.7}$$

where the coefficients $A_{mn}^{\pm}$ are related to the impedance tensors $a^{\pm}mn$ by the explicit formulas

$$\begin{pmatrix} A_{11}^{\pm} & A_{12}^{\pm} \\ A_{21}^{\pm} & A_{22}^{\pm} \end{pmatrix} = \frac{1}{a_{21}^{\pm}}\begin{pmatrix} a_{12}^{\pm}a_{21}^{\pm}-a_{11}^{\pm}a_{22}^{\pm} & a_{11}^{\pm} \\ -a_{22}^{\pm} & 1 \end{pmatrix} \tag{2.8}$$

presented, for example, in [18]. Finally, fields $\Phi_n(r,\theta)$ have to satisfy conditions at infinity, which require that they do not contain any waves arriving to the wedge $\alpha_- < \theta < \alpha_+$, except for the incident waves

$$\Phi_1(r,\theta)=p_h\mathrm{e}^{-\mathrm{i}r\cos(\theta-\theta_0)}, \quad \Phi_2(r,\theta)=p_e\mathrm{e}^{-\mathrm{i}r\cos(\theta-\theta_0)} \tag{2.9}$$

with the coefficients p_e and p_h from (2.3).

Next, we introduce new unknowns $U_1(r,\theta)$ and $U_2(r,\theta)$ related to $\Phi_1(r,\theta)$ and $\Phi_2(r,\theta)$ by

$$U_1=\Phi_1+\mathrm{i}\Phi_2, \qquad \Phi_1=\frac{1}{2}(U_1+U_2)$$
$$U_2=\Phi_1-\mathrm{i}\Phi_2, \qquad \Phi_2=\frac{1}{2\mathrm{i}}(U_1-U_2) \tag{2.10}$$

and satisfying the Helmholtz equations

$$\nabla^2 U_n(r,\theta)+U_n(r,\theta)=0, \qquad n=1,2 \tag{2.11}$$

complemented by the boundary conditions

$$\pm\mathrm{i}\left(\frac{1}{r}\frac{\partial U_1}{\partial\theta}-\mathrm{i}\cos\beta\frac{\partial U_1}{\partial r}\right)+q_{11}^{\pm}U_1+q_{12}^{\pm}U_2=0, \quad \theta=\alpha_{\pm} \tag{2.12}$$

$$\pm\mathrm{i}\left(\frac{1}{r}\frac{\partial U_2}{\partial\theta}+\mathrm{i}\cos\beta\frac{\partial U_2}{\partial r}\right)+q_{21}^{\pm}U_1+q_{22}^{\pm}U_2=0, \quad \theta=\alpha_{\pm} \tag{2.13}$$

with the coefficients

$$q_{11}^{\pm}=\frac{1}{2}\left[A_{11}^{\pm}+A_{22}^{\pm}-\mathrm{i}A_{12}^{\pm}+\mathrm{i}A_{21}^{\pm}\right]$$
$$q_{12}^{\pm}=\frac{1}{2}\left[A_{11}^{\pm}-A_{22}^{\pm}+\mathrm{i}A_{12}^{\pm}+\mathrm{i}A_{21}^{\pm}\right]$$
$$q_{21}^{\pm}=\frac{1}{2}\left[A_{11}^{\pm}-A_{22}^{\pm}-\mathrm{i}A_{12}^{\pm}-\mathrm{i}A_{21}^{\pm}\right]$$
$$q_{22}^{\pm}=\frac{1}{2}\left[A_{11}^{\pm}+A_{22}^{\pm}+\mathrm{i}A_{12}^{\pm}-\mathrm{i}A_{21}^{\pm}\right] \tag{2.14}$$

and by the conditions at infinity, which require that $U_1(r,\theta)$ and $U_2(r,\theta)$ do not contain any waves arriving to the wedge $\alpha_- < \theta < \alpha_+$ from infinity, except for the plane waves

$$U_n^0(r,\theta)=T_n\mathrm{e}^{-\mathrm{i}r\cos(\theta-\theta_0)} \tag{2.15}$$

with the coefficients

$$T_1=p_h+\mathrm{i}p_e, \qquad T_2=p_h-\mathrm{i}p_e \tag{2.16}$$

explicitly determined by the parameters p_e and p_h from (2.3).

Before proceeding to the solution of the problem (2.11)–(2.14) in the general case with an arbitrary skew angle β and with arbitrary (physically admissible) coefficients $q_{mn}^{\pm}$ it is instructive to mention some special cases which admit conventional analytic solutions.

In the most simple case, characterized by the identities $\beta = 90^\circ$ and $q_{12}^{\pm}=q_{21}^{\pm}=0$, the problem splits into two independent scalar problems with respect to the functions U_n which have to obey the boundary conditions

$$\mp\frac{1}{r}\frac{\partial U_n}{\partial\theta}+\mathrm{i}q_{nn}^{\pm}U_n=0, \qquad \theta=\alpha_{\pm}, \quad n=1,2. \tag{2.17}$$

Such problems essentially coincide with the scalar problem of diffraction by a wedge with impedance boundary conditions, and they can be easily solved by the Sommerfeld–Maliuzhinets method [19].

Slightly more difficult problems arise when the matrices $q_{mn}^{\pm}$ are still diagonal but the skew incident angle β has an arbitrary value. In this case the problem (2.11)–(2.14) also splits into independent scalar problems with respect to the functions U_n satisfying the boundary conditions

$$\mp\frac{1}{r}\frac{\partial U_n}{\partial\theta}\mp(-1)^n\mathrm{i}\cos\beta\frac{\partial U_n}{\partial r}+\mathrm{i}q_{nn}^{\pm}U_n=0, \quad \theta=\alpha_{\pm}, \ n=1,2 \tag{2.18}$$

which differ from (2.17) by the presence of the radial derivatives. Such problems can also be easily solved by the Sommerfeld–Maliuzhinets method or by its extensions, discussed for example in [8].

Even more generally, a conventional close-form analytic solution of the problem (2.11)–(2.14) can be obtained in any case where the matrices $q^{\pm}_{mn}$ are triangular, so that either of the identities $q^{\pm}_{12} = 0$ or $q^{\pm}_{21} = 0$ is valid. Indeed, assuming for definiteness that $q^{\pm}_{12} = 0$ we first compute U_1 as the solution of the scalar problem with the boundary conditions of the type (2.18). Then, the second unknown U_2 can be determined from a similar problem with inhomogeneous boundary conditions

$$\mp\frac{1}{r}\frac{\partial U_2}{\partial\theta} \mp \mathrm{i}\cos\beta\frac{\partial U_2}{\partial r} + \mathrm{i}q^{\pm}_{22}U_2 = -\mathrm{i}q^{\pm}_{21}U_1, \quad \theta = \alpha_{\pm}. \tag{2.19}$$

Such problems can also be solved by the Sommerfeld–Maliuzhinets method and by its extensions.

It should also be emphasized that the above mentioned specific classes of configurations do not exhaust all elementary cases when the considered problem of diffraction admits conventional closed-form analytic solutions. In particular, in the case of normal incidence the problem of diffraction can be solved analytically whenever the matrices $A^{\pm}_{mn}$ from (2.6), (2.7) are diagonal or triangular. For example, if $\cos\beta = A^{\pm}_{12} = A^{\pm}_{21} = 0$, then (2.6), (2.7) are reduced to uncoupled impedance boundary conditions

$$\mp\frac{1}{r}\frac{\partial\Phi_n}{\partial\theta} + \mathrm{i}A^{\pm}_{nn}\Phi_n = 0, \qquad \theta = \alpha_{\pm}, \quad n = 1,2 \tag{2.20}$$

which make it possible to solve the problem (2.5)–(2.9) directly by the Maliuzhinets method, without conversion to the form (2.11)–(2.14). It is instructive to observe that in this case the matrix $q^{\pm}_{mn}$ from (2.14) has the symmetric structure

$$q^{\pm} = \frac{1}{2}\begin{pmatrix} A^{\pm}_{11} + A^{\pm}_{22}, & A^{\pm}_{11} - A^{\pm}_{22} \\ A^{\pm}_{11} - A^{\pm}_{22}, & A^{\pm}_{11} + A^{\pm}_{22} \end{pmatrix} \tag{2.21}$$

which is not necessarily diagonal and, therefore, does not guarantee analytic solvability of the problem (2.11)–(2.14) obtained from (2.5)–(2.9) by the transformation (2.10).

III. Structure of the Solution to the General Problem

Elementary analysis of the problem (2.11)–(2.14) suggests that its solution admits the decomposition

$$U_n(r,\theta) = U^g_n(r,\theta) + u_n(r,\theta)\mathrm{e}^{\mathrm{i}r}, \qquad n = 1,2 \tag{3.1}$$

into the geometric components $U^g_n(r,\theta)$ and the diffracted components $U^d_n(r,\theta) = u_n(r,\theta)\mathrm{e}^{\mathrm{i}r}$.

The geometric field $U^g_n(r,\theta)$ consists of the incident wave and a finite number of reflected waves, which can be computed by explicit algebraic formulas. To avoid emphasis on material that is not essential for our purposes here, we restrict ourselves henceforth to particular but rather representative configurations (see Fig. 2) characterized by the constraints

$$\alpha_- = 0, \quad \alpha_+ > \pi, \qquad \theta_0 + \pi < \alpha_+ \tag{3.2}$$

which guarantee the absence of multiple-reflected waves and lead to the representation

$$U^g_n(r,\theta) = \chi_2(\theta)T_n\mathrm{e}^{-\mathrm{i}r\cos(\theta-\theta_0)} + \chi_1(\theta)R_n\mathrm{e}^{-\mathrm{i}r\cos(\theta+\theta_0)} \qquad n = 1,2 \tag{3.3}$$

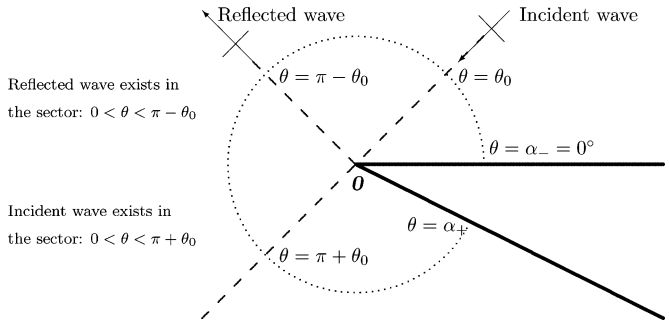

Fig. 2. Geometry of the problem on the (r,θ)-plane.

where T_n are the pre-defined parameters from (2.16), R_n are the reflection coefficients determining the amplitude and polarization of the reflected waves, and

$$\chi_m(\theta) = \begin{cases} 1, & \text{if } \theta < \theta_m \\ 0, & \text{otherwise} \end{cases} \tag{3.4}$$

are step-functions with the parameters

$$\theta_1 = \pi - \theta_0, \qquad \theta_2 = \pi + \theta_0. \tag{3.5}$$

To compute the reflection coefficients R_n it suffices to consider an auxiliary problem of reflection of the plane wave (2.3) by the boundary of a half-space with a surface impedance coinciding with the impedance of the face $\theta = \alpha_-$. In other words, we consider a particular case of the problem (2.11)–(2.14) characterized by the conditions

$$\alpha_- = 0, \quad \alpha_+ = \pi, \quad q^{+}_{mn} = q^{-}_{mn}, \quad (m = 1,2, \quad n = 1,2). \tag{3.6}$$

The solution of the reflection problem (2.11)–(2.14), (3.6) has the structure

$$U_n(r,\theta) = T_n\mathrm{e}^{-\mathrm{i}r\cos(\theta-\theta_0)} + R_n\mathrm{e}^{-\mathrm{i}r\cos(\theta+\theta_0)}, \quad n = 1,2 \tag{3.7}$$

where T_n are known from (2.16) while the yet unknown quantities R_n must ensure that the pair $U_1(r,\theta)$ and $U_2(r,\theta)$ obeys the required boundary conditions. Then, a straightforward substitution of (3.7) into the boundary conditions (2.12), (2.13) simplified by the assumptions (3.6) leads to the system of algebraic equations

$$(\widehat{K}_0 + \widehat{K}_\beta)\circ\begin{bmatrix} R_1 \\ R_2 \end{bmatrix} = (\widehat{K}_0 - \widehat{K}_\beta)\circ\begin{bmatrix} T_1 \\ T_2 \end{bmatrix} \tag{3.8}$$

with the matrices

$$\widehat{K}_0 = \sin\theta_0\begin{bmatrix} 1 & 0 \\ 0 & 1 \end{bmatrix}$$
$$\widehat{K}_\beta = \begin{bmatrix} q^{-}_{11} & q^{-}_{12} \\ q^{-}_{21} & q^{-}_{22} \end{bmatrix} + \mathrm{i}\cos\beta\cos\theta_0\begin{bmatrix} 1 & 0 \\ 0 & -1 \end{bmatrix}. \tag{3.9}$$

Assuming that the matrix $\widehat{K}_0 + \widehat{K}_\beta$ is invertible, we finally get

$$\begin{bmatrix} R_1 \\ R_2 \end{bmatrix} = \widehat{K}\circ\begin{bmatrix} T_1 \\ T_2 \end{bmatrix}, \quad \widehat{K} = (\widehat{K}_0+\widehat{K}_\beta)^{-1}\circ(\widehat{K}_0-\widehat{K}_\beta) \tag{3.10}$$

where $\widehat{K}$ is a constant matrix that will be referred to as the "reflection matrix."

Since the geometric components $U^g_n(r,\theta)$ of the decompositions (3.1) satisfy the Helmholtz (2.5) automatically, the

diffracted components $U_n^d(r,\theta)$ should also obey this equation everywhere, except on the rays $\theta = \theta_1$ and $\theta = \theta_2$, where $U_n^g(r,\theta)$ is not continuous. Then, straightforward substitution of $U_n^d(r,\theta) = u_n(r,\theta)\mathrm{e}^{\mathrm{i}r}$ into (2.5) shows that $u_n(r,\theta)$ satisfies the "complete transport equation" $\nabla^2 u_n + 2\mathrm{i}\vec{\nabla}(r)\cdot\vec{\nabla}u_n + \mathrm{i}\nabla^2(r)u_n = 0$, which expands to

$$\left(\frac{\partial^2 u_n}{\partial r^2} + \frac{1}{r}\frac{\partial u_n}{\partial r} + \frac{1}{r^2}\frac{\partial^2 u_n}{\partial \theta^2}\right) + 2\mathrm{i}\frac{\partial u_n}{\partial r} + \mathrm{i}\frac{u_n}{r} = 0, \quad \theta \neq \theta_{1,2} \tag{3.11}$$

and can be further converted, by regrouping and multiplication by r^2, to an equivalent form

$$\frac{r^2}{2}\frac{\partial^2 u_n}{\partial r^2} + r\left(\frac{1}{2} + \mathrm{i}r\right)\frac{\partial u_n}{\partial r} + \frac{1}{2}\frac{\partial^2 u_n}{\partial \theta^2} + \frac{\mathrm{i}r u_n}{2} = 0, \quad \theta \neq \theta_{1,2} \tag{3.12}$$

which is proven to be more suitable than (3.11) for the analysis by the probabilistic method [3], [5]–[7]. Additionally, to maintain the smoothness of the total wave fields $U_n^g(r,\theta)$ from (3.1), the amplitudes $u_n(r,\theta)$ of the diffracted fields have to satisfy the interface conditions

$$u_n(r,\theta_1+0) - u_n(r,\theta_1-0) = R_n \tag{3.13}$$

$$u_n(r,\theta_2+0) - u_n(r,\theta_2-0) = T_n \tag{3.14}$$

$$\left.\frac{\partial u_n}{\partial \theta}\right|_{\theta=\theta_m+0} = \left.\frac{\partial u_n}{\partial \theta}\right|_{\theta=\theta_m-0}, \quad m = 1,2. \tag{3.15}$$

where T_n and R_n are the parameters from (3.7) explicitly defined by (2.16) and (3.10). Finally, the amplitudes $u_n(r,\theta)$ must obey the conditions at infinity $u_n(\infty,\theta) = 0$, where $\theta \neq \theta_{1,2}$, and these amplitudes have to be coupled by the boundary conditions

$$\mp\left(\frac{\partial u_1}{\partial \theta} - \mathrm{i}r\cos\beta\frac{\partial u_1}{\partial r}\right) + r\left[\mathrm{i}q_{11}^{\pm} \mp \cos\beta\right]u_1 + \mathrm{i}r q_{12}^{\pm}u_2 = 0 \qquad \theta = \alpha_{\pm} \tag{3.16}$$

$$\mp\left(\frac{\partial u_2}{\partial \theta} + \mathrm{i}r\cos\beta\frac{\partial u_2}{\partial r}\right) + r\left[\mathrm{i}q_{22}^{\pm} \pm \cos\beta\right]u_2 + \mathrm{i}r q_{21}^{\pm}u_1 = 0 \qquad \theta = \alpha_{\pm} \tag{3.17}$$

which take into account that the geometric components $U_n^g(r,\theta)$ of the wave fields (3.1) automatically satisfy the boundary conditions (2.12) and (2.13).

IV. Auxiliary Scalar Problem

Our approach to the vector problem (3.12)–(3.17) is based on a probabilistic solution of a scalar equation

$$\frac{r^2}{2}\frac{\partial^2 u}{\partial r^2} + r\left(\frac{1}{2} + \mathrm{i}r\right)\frac{\partial u}{\partial r} + \frac{1}{2}\frac{\partial^2 u}{\partial \theta^2} + \frac{\mathrm{i}r u}{2} = 0 \tag{4.1}$$

considered in a wedge $\alpha_- < \theta < \alpha_+$ with the interface conditions

$$u(r,\theta_1+0) - u(r,\theta_1-0) = R, \quad R = \mathrm{const} \tag{4.2}$$

$$u(r,\theta_2+0) - u(r,\theta_2-0) = T, \quad T = \mathrm{const} \tag{4.3}$$

$$u'_\theta(r,\theta_m+0) - u'_\theta(r,\theta_m-0) = 0, \quad m = 1,2 \tag{4.4}$$

assigned on the interior rays $\theta = \theta_m \in (\alpha_-, \alpha_+)$, and with the boundary condition

$$\mp\frac{\partial u}{\partial \theta} + L\frac{\partial u}{\partial r} + Bu + \gamma(f-u) = 0, \quad \theta = \alpha_{\pm}, \quad (\gamma = \mathrm{const} > 0) \tag{4.5}$$

where $B \equiv B(r,\alpha_\pm)$, $L \equiv L(r,\alpha_\pm)$ and $f \equiv f(r,\alpha\pm)$ are functions on the faces of the wedge.

Equation (4.1) together with the interface and boundary conditions (4.2)–(4.5) belong to a class of problems discussed in [7], and the straightforward application of the technique described in [14] leads to the formula

$$u(r,\theta) = \mathbf{E}\left\{f(\xi_\tau,\eta_\tau)Q_t + \sum_{\nu=1}^{t_\nu<\tau}\Omega_\nu(R,T)Q_{\tau_\nu}\right\} \tag{4.6}$$

where

$$Q_t = \exp\left(\frac{1}{2}\int_0^\tau \mathrm{i}\xi_s \mathrm{d}s + \int_0^\tau B(\xi_s,\eta_s)\mathrm{d}\lambda_s\right) \tag{4.7}$$

and $\mathbf{E}$ denotes the mathematical expectation computed over the stochastic processes ξ_t, η_t, τ, t_ν, and Ω_ν controlled by the rules described below.

The angular motion η_t starts from $\eta_0 = \theta$ and is controlled by the stochastic equations

$$\eta_0 = \theta, \qquad \mathrm{d}\eta_t = \begin{cases} \mathrm{d}w_t^2, & \text{if } \eta_t \neq \alpha_\pm \\ \mp\mathrm{d}t, & \text{if } \eta_t = \alpha_\pm \end{cases} \tag{4.8}$$

driven by the standard one-dimensional Brownian motion w_t^2, which is also known as the Wiener process and is intensively studied in the literature [11], [13]–[16], [28]. Equations (4.8) show that η_t behaves as a Brownian motion inside the interval (α_-,α_+), but when η_t reaches one of the boundary points $\eta = \alpha_\pm$ it is deterministically reflected back. The radial motion ξ_t starts at $t = 0$ from $\xi_0 = r$ and is controlled by the stochastic equation

$$\xi_0 = r, \quad \mathrm{d}\xi_t = \begin{cases} \xi_t \mathrm{d}w_t^1 + \xi_t\left(\frac{1}{2} + \mathrm{i}\xi_t\right)\mathrm{d}t, & \text{if } \eta_t \neq \alpha_\pm \\ L(\xi_t,\eta_t)\mathrm{d}t, & \text{if } \eta_t = \alpha_\pm \end{cases} \tag{4.9}$$

driven by the Brownian motion w_t^1 independent of the motion w_t^2 from (4.8).

The angular motion η_t is not only involved in (4.6) and (4.7) as an argument in $u(\xi_t,\eta_t)$ and $B(\xi_t,\eta_t)$, but it also affects these formulas through the "local time" λ_t which can be introduced as the integral $\lambda_t = \int_0^t \mathrm{d}\lambda_s$ with respect to the measure

$$\mathrm{d}\lambda_t = \begin{cases} 0, & \text{if } \eta_t \neq \alpha_\pm \\ \mathrm{d}t, & \text{if } \eta_t = \alpha_\pm. \end{cases} \tag{4.10}$$

The local time λ_t determines the "swap time" τ which is a random number distributed as

$$\mathbf{P}(\lambda_t \leq \lambda_\tau < \lambda_t + \mathrm{d}\lambda_t) = \gamma\mathrm{d}\lambda_t \tag{4.11}$$

where γ is a parameter from (4.5). Obviously, (4.11) means that λ_τ has a Poisson distribution with respect to the local time λ_t.

Since the angular motion η_t runs inside the interval (α_-, α_+) as a standard Brownian motion, it crosses infinitely many times the points $\eta = \theta_1$ and $\eta = \theta_2$ where the interface conditions (4.2)–(4.4) are assigned. The consecutive crossings of either of these points can be enumerated by the integer $\nu \geq 1$ which is used as a summation index in (4.6). Correspondingly, t_ν denotes the time when the νth crossing takes place, and the factor $\Omega_\nu(R,T)$ is computed by the rule

$$\Omega_\nu(R,T) = \begin{cases} R, & \text{if } \eta_t = \theta_1 \text{ and } \eta_{t+0} < \theta_1 < \eta_{t-0} \\ -R, & \text{if } \eta_t = \theta_1 \text{ and } \eta_{t-0} < \theta_1 < \eta_{t+0} \\ T, & \text{if } \eta_t = \theta_2 \text{ and } \eta_{t+0} < \theta_2 < \eta_{t-0} \\ -T, & \text{if } \eta_t = \theta_2 \text{ and } \eta_{t-0} < \theta_2 < \eta_{t+0} \\ 0, & \text{otherwise} \end{cases} \tag{4.12}$$

where it is assumed, for brevity, that $t = t_\nu$.

V. Solution of the Vector Problem of Diffraction

To apply the auxiliary scalar solutions from the previous section to the main vector problem (3.12)–(3.17) we observe that the (3.12) can be treated as two independent scalar equations similar to (4.1). Likewise, the interface conditions (3.13)–(3.15) split into the case of independent scalar conditions with respect to the unknowns $u_1(r,\theta)$ and $u_2(r,\theta)$. As for the boundary conditions (3.16) and (3.17) which, in general, can not be decoupled, we rearrange them as

$$\mp \frac{\partial u_1}{\partial \theta} + L_1 \frac{\partial u_1}{\partial r} + B_1 u_1 + \gamma_1(\mathrm{e}^{\mathrm{i}\phi_1} u_2 - u_1) = 0 \qquad \theta = \alpha_\pm \tag{5.1}$$

$$\mp \frac{\partial u_2}{\partial \theta} + L_2 \frac{\partial u_2}{\partial r} + B_2 u_2 + \gamma_2(\mathrm{e}^{\mathrm{i}\phi_2} u_1 - u_2) = 0 \qquad \theta = \alpha_\pm \tag{5.2}$$

where

$$\gamma_1(r,\alpha_\pm) = \left|rq_{12}^\pm\right|, \quad \phi_1(r,\alpha_\pm) = \arg\left[\mathrm{i}rq_{12}^\pm\right] \tag{5.3}$$

$$\gamma_2(r,\alpha_\pm) = \left|rq_{21}^\pm\right|, \quad \phi_2(r,\alpha_\pm) = \arg\left[\mathrm{i}rq_{21}^\pm\right] \tag{5.4}$$

and

$$\begin{aligned} B_1(r,\alpha_\pm) &= r\left[\mathrm{i}q_{11}^\pm \mp \cos\beta\right] + \gamma_1(r,\alpha_\pm) \\ L_1(r,\alpha_\pm) &= \pm \mathrm{i}r\cos\beta \end{aligned} \tag{5.5}$$

$$\begin{aligned} B_2(r,\alpha_\pm) &= r\left[\mathrm{i}q_{22}^\pm \pm \cos\beta\right] + \gamma_2(r,\alpha_\pm) \\ L_2(r,\alpha_\pm) &= \mp \mathrm{i}r\cos\beta. \end{aligned} \tag{5.6}$$

To compute $u_1(r,\theta)$ we treat $u_2(r,\theta)$ as if it were known, and applying the results of the previous sections we get

$$u_1(r,\theta) = \mathbf{E}\left\{u_2\left(\xi_{\tau_1},\eta_{\tau_1}\right)\mathrm{e}^{\mathrm{i}\mu_1 + S_1(\tau_1)} + \sum_{\nu=1}^{t_\nu<\tau_1} \Omega_\nu(R_1,T_1)\mathrm{e}^{S_1(t_\nu)}\right\} \tag{5.7}$$

where λ_t, τ_1 are the local and the swap times defined by (4.10), (4.11) with $\gamma = \gamma_1$, and

$$\mu_1 = \phi_1\left(\xi_{\tau_1},\eta_{\tau_1}\right), \quad S_1(t) = \frac{1}{2}\int_0^t \mathrm{i}\xi_s \mathrm{d}s + \int_0^t B_1(\xi_s,\eta_s)\mathrm{d}\lambda_s \tag{5.8}$$

are the functionals defined on the trajectories of the random motions ξ_t, η_t. It is clear that the only thing in the right-hand side of (5.7) which is not yet defined is $u_2(\xi_{\tau_1},\eta_{\tau_1})$, but it is also clear that this function can be computed in terms of u_1 by the Feynman–Kac formulas (4.6) which leads to the expression

$$u_2\left(\xi_{\tau_1},\eta_{\tau_1}\right) = \mathbf{E}\left\{u_1\left(\xi_{\tau_2},\eta_{\tau_2}\right)\mathrm{e}^{\mathrm{i}\mu_2 + S_2(\tau_2)} + \sum_{\tau_1<t_\nu<\tau_2} \Omega_\nu(R_2,T_2)\mathrm{e}^{S_2(t_\nu)}\right\} \tag{5.9}$$

where

$$\mu_2 = \phi_2\left(\xi_{\tau_2},\eta_{\tau_2}\right), \quad S_2(t) = \frac{1}{2}\int_{\tau_1}^t \mathrm{i}\xi_s \mathrm{d}s + \int_{\tau_1}^t B_2(\xi_s,\eta_s)\mathrm{d}\lambda_s. \tag{5.10}$$

Next we substitute (5.9) into (5.7) and observe that the right-hand side of the resulting expression contains the value $u_1(\xi_{\tau_2},\eta_{\tau_2})$ which is not yet known, but it can be computed by a formula similar to (5.9). It is obvious that the iterations may be continued indefinitely and that they may be started from either of the functions u_1 or u_2. As a result we eventually arrive at the solution of the problem in the form

$$u_m(r,\theta) = \mathbf{E}\left\{\sum_{\nu=1}^\infty \Omega_\nu\left(R_{\Lambda(t_\nu)},T_{\Lambda(t_\nu)}\right)\mathrm{e}^{S(t_\nu)}\right\} \qquad m = 1,2 \tag{5.11}$$

$$S(t) = \frac{1}{2}\int_0^t \mathrm{i}\xi_s \mathrm{d}s + \int_0^t B_{\Lambda(s)}(\xi_s,\eta_s)\mathrm{d}\lambda_s + \sum_{n=1}^{\tau_n<t} \phi_{\Lambda(\tau_n)}\left(\xi_{\tau_n},\eta_{\tau_n}\right) \tag{5.12}$$

which employs averaging over the random processes ξ_t, η_t and $\Lambda(s)$ as described below.

The most important component of the solution (5.11) is the angular random motion η_t which starts at $t = 0$ from the observation point $\eta_0 = \theta$ and is controlled by the stochastic (4.8). This motion runs inside the interval (α_-, α_+) crossing the interfaces $\eta = \theta_1$ and $\eta = \theta_2$ at the times t_n with $n \geq 0$. The angular random motion determines two other random processes, namely: the local time λ_t introduced as the integral $\lambda_t = \int_0^t \mathrm{d}\lambda_s$ with respect to the measure (4.10) and $0 < \tau_1 < \tau_2 < \ldots$ are the swap times which are random numbers distributed according to

$$\mathbf{P}(\lambda_t \leq \lambda_\tau < \lambda_t + \mathrm{d}\lambda_t) = \gamma_{\Lambda(t)}\mathrm{d}\lambda_t \tag{5.13}$$

where the index $\Lambda(t)$ is determined by the rules

$$\Lambda(0) = m, \quad \Lambda(t+0) - \Lambda(t) = \begin{cases} 0, & \text{if } t \neq \tau_\mu \\ (-1)^{m+\mu}, & \text{if } t = \tau_\mu \end{cases} \tag{5.14}$$

which state that $\Lambda(t)$ starts from the initial index $\Lambda(0) = m$ from the left side of (5.11) and switches to another index at every swap time $t = \tau_\mu$. Finally, the radial motion ξ_t is controlled by the equation

$$\xi_0 = r, \quad \mathrm{d}\xi_t = \begin{cases} \xi_t \mathrm{d}w_t^1 + \xi_t\left(\frac{1}{2} + \mathrm{i}\xi_t\right)\mathrm{d}t, & \text{if } \eta_t \neq \alpha_\pm \\ L_{\Lambda(t)}(\xi_t,\eta_t)\mathrm{d}t, & \text{if } \eta_t = \alpha_\pm \end{cases} \tag{5.15}$$

with the upper line describing the evolution of ξ_t while the angular motion η_t is located inside the wedge $\alpha_- < \eta < \alpha_+$, and with the bottom line describing the deterministic shift of ξ_t at the time when the angular motion η_t is located on one of the boundaries $\eta = \alpha_\pm$.

VI. Discussion of the Solution

Formula (5.11) represents the exact solution of the diffraction problem in the same rigorous sense as the Sommerfeld integral describes diffraction by an ideally reflecting half-plane. However, compared to conventional closed-form solutions, the probabilistic expression (5.11) has a disadvantage caused by the use of mathematical tools that are not common in the theory of wave propagation, and, therefore, which do not have an established reputation of practicability. For this reason we briefly discuss here key elements of the solution (5.11) with emphasis on the aspects which may be employed for numerical evaluation of the probabilistic solution (5.11) of the problem of diffraction.

The most important component of Ito's stochastic differential (4.8) and (5.15) is the one-dimensional Brownian motion w_t known also as the Wiener process.

Suppose a particle moves along the real axis $-\infty < x < \infty$ starting at the time $t = 0$ from $x = 0$ and jumping at the instants $t_n = n\Delta t$ the distance ϵ in either of two equally probable directions. Then, the particle's position x_n in the time interval $[t_n, t_{n+1})$ prior to the $(n+1)$th jump is represented by the sum $x_n = \sum_{\nu=1}^{n} \Delta x_\nu$ of independent random variables $\Delta x_n = \pm\epsilon$ with two equally probable values. The sequences x_n and t_n determine a piecewise constant function $\widetilde{w}_t = x_{\tilde{t}}$, where $\tilde{t}$, is the last instant of the series t_n preceding or coinciding with t. It is well known [10], [11], [32] that if the time and space meshes decrease together as $\Delta t = \epsilon^2 \to 0$, then the jump-motion $\widetilde{w}_t$ converges to a continuous random motion w_t known as the one-dimensional Brownian motion. As for the Brownian motion in $\mathbb{R}^N$ it can be introduced as a superposition $\vec{w}_t = (w_t^1, w_t^2, \ldots, w_t^N)$ of one-dimensional Brownian motions along each of the Cartesian axes.

The above definition of the Brownian motion can be straightforwardly generalized to a description of the Brownian motion with a drift which plays an important role in the probabilistic solutions of differential equations. Let $\sigma(x)$ and $A(x)$ be some functions and let η_t be a discrete random motion launched from x and consisting of the jumps

$$\eta_t \longrightarrow \xi_{t+\Delta t} = \eta_t + \sigma(\eta_t)\Delta w + A(\eta_t)\Delta t, \quad \Delta w = \pm\sqrt{\Delta t} \tag{6.1}$$

where Δw is the Brownian displacement on the time interval Δt. Then, passing to the limit $\Delta t \to 0$, which is possible under some mild conditions on $A(x)$ and $\sigma(x)$, we get a continuous random motion η_t which is considered as a solution of the stochastic differential equation

$$\mathrm{d}\eta_t = \sigma(\eta_t)\mathrm{d}w_t + A(\eta_t)\mathrm{d}t. \tag{6.2}$$

It is clear from (6.1) that the jump $\Delta\eta_t$ can be considered as a superposition of the deterministic move $\Delta\zeta_t = A(\eta_t)\Delta t$ and of the random displacement $w_{\Delta t}$. Due to this interpretation, any solution of (6.2) is commonly referred to as a Brownian motion with a drift.

An attractive feature of (6.2) is its versatility, which makes it possible to include into consideration compound equations like (4.8) and (5.15). For example, (4.8), which controls the angular motion η_t, can be considered as a particular case of (6.2) with the coefficients

$$\sigma(\eta) = \begin{cases} 1, & \text{if } \alpha_- < \eta < \alpha_+ \\ 0, & \text{if } \eta = \alpha_\pm \end{cases}$$
$$A(\eta) = \begin{cases} 0, & \text{if } \alpha_- < \eta < \alpha_+ \\ \mp 1, & \text{if } \eta = \alpha_\pm. \end{cases} \tag{6.3}$$

The approximation (6.1) is usually referred to as the Euler approximation of the stochastic differential (6.2), and it can be used as a practical scheme for the numerical solution of stochastic equations like (6.2). Similarly to the Euler scheme from the theory of ordinary differential equations, the stochastic Euler scheme is very simple for understanding and implementation, but it's rate of convergence is not always sufficient for practical needs. In cases when higher computational efficiency is required, a more accurate scheme should be used. In recent years a number of high-order schemes of numerical integration of stochastic differential equations have been developed, and many of them are presented in the monographs [12], [22], which also contain computer codes and intensive bibliographies.

It should also be mentioned that the Brownian motion may be approximated by a method radically different than that outlined above. For example, it is known (see detail in [14], [16]) that if $a_0, a_1, \ldots,$ is a series of independent Gaussian random numbers with zero mean and unit covariance, then the series

$$w_t = a_0 t + \frac{\sqrt{2}}{\pi}\sum_{n=1}^{\infty}\left(\sum_{k=2^{n-1}}^{2^n-1} a_k \frac{\sin(k\pi t)}{k}\right), \quad 0 \le t \le 1 \tag{6.4}$$

uniformly converges to the standard Brownian motion. This representation makes it possible to parameterize solutions of the stochastic (6.2) by a vector $(a_0, a_1, a_2, \ldots)$ from the infinite-dimensional space. Correspondingly, truncations of this vector generate sets of specific samples of the Brownian motion parameterized by a finite number of parameters.

Replacement of the random motions ξ_t and η_t by their approximations is not the only source of numerical error in the probabilistic expression (5.11). Computation of the mathematical expectation is another element which, in general, can not be computed without error. An obvious method to estimate the mathematical expectation is to compute the functional from (5.11) along a large number of sample trajectories of the random motions involved, and then compute the average. This approach, based on the central limit theorem, is intuitively the simplest, but it converges only at the rate $D/\sqrt{N}$ where D is a covariance of statistical data and N is the number of averaged samples. If the covariance is sufficiently small, then the error may be tolerable even for moderate N, and if the variance is bigger, it may often be significantly reduced by "variance reduction techniques," described, for example, in [12], [22]. It should also be mentioned that the mathematical expectations like (5.11) can be computed by deterministic methods. Some of these methods [23], [29], [31] are based on quasi-Monte Carlo simulations which are similar to Monte Carlo methods but have a better rate of convergence $O(\log^k(N)/N$. Another group of

the methods presented in [9], [17], [24] treats the mathematical expectation over the trajectories of the Brownian motions as an integral in an infinite dimensional space with the Gaussian measure and develop quadrature rules similar to those used in the classical finite-dimensional integration.

The above remarks suggest that development of practical methods for evaluation of probabilistic formulas like (5.11) should be considered as an important topic of further research which deserves to be studied independently of a particular problem of wave propagation, similarly to how the methods of computation of the Sommerfeld integrals [30] and Maliuzhinets function [19] have been developed separately from the research where these tools are used for representation of wave fields.

VII. Numerical Examples

To illustrate the feasibility of the probabilistic solution of the diffraction problem we conducted a series of numerical experiments aimed at testing critical components of the developed method which were not already tested in the previous publication dealing with the simpler scalar problem of diffraction [7].

To plan the experiments which provide real testing of the approach without overshadowing crucial points by the bulk of numbers it is important to identify the components of the obtained solution which were not tested before. We observe that there are only two noticeable differences between the probabilistic solution of the vector problem (3.12)–(3.17) and the similar solution of the pair of independent scalar problems which arise from (3.12)–(3.17) after the replacement of the coupled boundary conditions (3.16), (3.17) by uncoupled conditions (2.17). Indeed, in that degenerate case, with the imposed constraints $\cos\beta = 0$ and $q_{12}^{\pm} = q_{21}^{\pm} = 0$, the solution (5.11)–(5.15) is simplified to the form

$$u_m(r,\theta) = \mathbf{E}\left\{\sum_{\nu=1}^{\infty}\Omega_\nu\left(R_m, T_m\right) \times \exp\left(\frac{1}{2}\int_0^t \mathrm{i}\xi_s \mathrm{d}s + \int_0^t B_m(\xi_s,\eta_s)\mathrm{d}\lambda_s\right)\right\}, \quad m=1,2 \tag{7.1}$$

where the radial motion ξ_t is controlled by the stochastic equation

$$\mathrm{d}\xi_t = \xi_t \mathrm{d}w_t^1 + \xi_t\left(\frac{1}{2} + \mathrm{i}\xi_t\right)\mathrm{d}t. \quad \xi_0 = r. \tag{7.2}$$

Direct comparison of the expressions (5.11)–(5.15) with (7.1), (7.2) makes it clear that the constraint $\cos\beta = 0$ affects the solution only through the structure of the radial motion ξ_t, which in the general case $\cos\beta \neq 0$ is governed by the stochastic (5.15) generalizing (7.2). Similarly, the coefficients $q_{12}^{\pm}$ and $q_{21}^{\pm}$ contribute to the general solution only through the two-valued random process $\Lambda(t)$, which is controlled by (5.13), (5.14), and which remains constant if $q_{12}^{\pm} = q_{21}^{\pm} = 0$.

The above observations show that testing the general solution can be subdivided into two independent tasks. To test the part of the solution that handles the complications caused by the inequality $\cos\beta \neq 0$ it suffices to limit the testing to configurations with diagonal matrices $q_{mn}^{\pm}$. Moreover, since the diagonal structure of these matrices splits the problem into two similar uncoupled problems, the test may not be less conclusive if it is limited to the computation of only one of the unknown functions corresponding to only one of the polarizations. Similarly, to test the part of the solution which handles coupling caused by the inequalities $q_{12}^{\pm} \neq 0$ and $q_{21}^{\pm} \neq 0$ it suffices to limit the testing to cases of normal incidence, i.e., when $\cos\beta = 0$. In particular, it suffices to consider the problem (3.12)–(3.17) with $\beta = 90°$ and with the matrices $q^{\pm}$ of the structure (2.21).

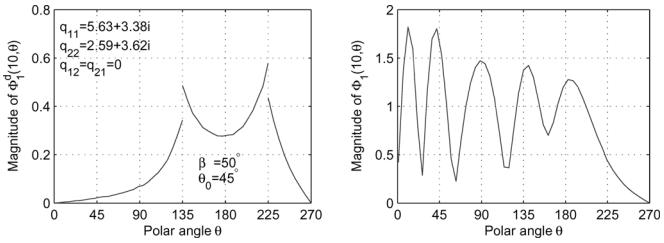

Fig. 3. Simulated total wave fields $\Phi_1(r,\theta)$ and its diffracted component $\Phi_1^d(r,\theta)$.

Our first numerical experiment deals with the problem in a wedge $0° < \theta < 270°$ exposed to a skew plane incident wave with the skew angle β, and with incidence angle $\theta_0 = 45°$. In this configuration the shadow domain $225° < \theta < 270°$ is illuminated only by diffracted waves, the sector $135° < \theta < 225°$ is accessible to the incident and diffracted waves, and the domain $\theta < 135°$ is exposed to the incident, reflected and diffracted waves. In this experiment we tested the handling of the skew incidence, and for this reason we assume that $\beta = 50°$ with the matrices $q^{\pm}$ from (3.16), (3.17) having the diagonal structure

$$q^{\pm} = \begin{pmatrix} 5.63 + 3.38\mathrm{i} & 0 \\ 0 & 2.59 + 3.62\mathrm{i} \end{pmatrix} \tag{7.3}$$

which is chosen because it corresponds to the problem considered in [18] analytically, by a modification of the Maliuzhinets method.

The results of the numerical simulations are shown in Fig. 3 where the right diagram shows the total field $\Phi_1(r,\theta)$ and the left diagram shows its diffracted component $\Phi_1^d(r,\theta)$ computed along the circle $r = 10$. All computations employed the averaging of 1500 random walks with the time increment $\Delta t = 0.01$. The infinite series in (5.11) was truncated after three consecutive new terms were smaller than 10^{-3}. The covariances of the statistical simulations did not exceed the level $D = 0.5$, which indicates high stability and good convergence of the method as the number N of averaged paths increases. It is obvious that our graph for the diffracted field agrees with the similar graph from [18, Fig. 3c], which is plotted with respect to the "Azimuth angle ϕ" related by the formula $\phi = 135° - \theta$ to the polar angle θ used here.

The second series of numerical experiments deals with the configuration used in [25] for validation of the semi-analytic "hybrid technique for the analysis of scattering by impedance wedges." This technique covered problems of diffraction of a plane wave skew incident on the wedge with isotropic impedance boundary conditions. Although such a problem is less general than those with anisotropic impedances considered here, it also does not have a known closed-form solution, and in [25] the obtained series approximation was tested on a special case of normal incidence, which admits an analytic solution.

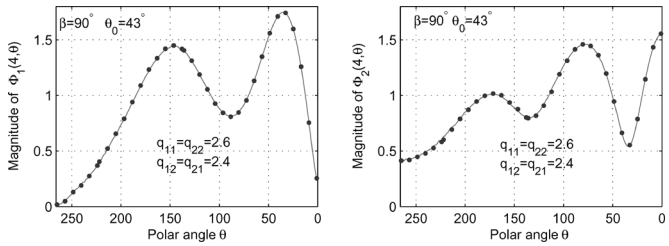

Fig. 4. Simulated total wave fields $\Phi_1(r,\theta)$ in the case (7.5).

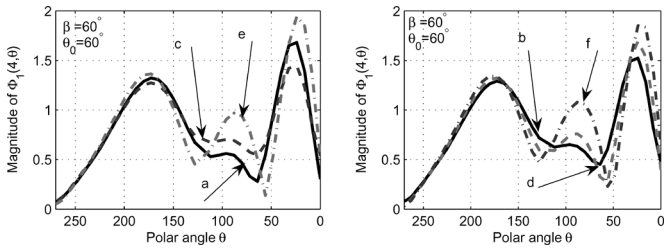

Fig. 5. Simulated total wave fields $\Phi_1(r,\theta)$ in general configurations.

Following [25] we considered a problem of diffraction in a wedge $0^\circ < \theta < 266^\circ$ for which both faces have isotropic impedances characterized by the constant tensors

$$A^+ = A^- = \begin{pmatrix} \rho & 0 \\ 0 & \frac{1}{\rho} \end{pmatrix}, \quad \rho = 5. \tag{7.4}$$

The incident plane wave was characterized by the polarization $p_h = 1$, $p_e = 0$, by the incidence angle $\theta_0 = 43^\circ$ and by the skew angle $\beta = 90^\circ$. In this configuration the shadow domain $223^\circ < \theta < 266^\circ$ is illuminated only by the diffracted waves, the domain $137^\circ < \theta < 223^\circ$ is exposed to the diffracted and reflected waves, and the sector $0^\circ < \theta < 137^\circ$ is accessible to the incident, reflected and diffracted waves.

As mentioned above this simple isotropic configuration is ideally suited for thorough testing of the most sophisticated part of the developed technique, which is the mechanism for handling coupling between two unknown functions through the boundary conditions (3.16), (3.17). Indeed, as mentioned in the end of Section II, matrices $q^\pm$ from (2.14) corresponding to (7.4) have the structure

$$q^+ = q^- = \frac{1}{2}\begin{pmatrix} \rho + \frac{1}{\rho}, & \rho - \frac{1}{\rho} \\ \rho - \frac{1}{\rho}, & \rho + \frac{1}{\rho} \end{pmatrix} = \begin{pmatrix} 2.6, & 2.4 \\ 2.4, & 2.6 \end{pmatrix} \tag{7.5}$$

which is neither diagonal nor triangular and, therefore, does not eliminate coupling in the boundary conditions of the problem (2.11)–(2.14). As a result, our numerical procedure, when solving exactly this truly vector problem, encounters all the principle difficulties caused by the coupling of electric and magnetic fields. On the other hand, if the tensors $A^\pm$ have the diagonal structure (7.4), then, as indicated in the end of Section II, the coupled problem (2.11)–(2.14) is equivalent to the uncoupled problem (2.5)–(2.9) which can be analytically solved by the Maliuzhinets method, as well as by the scalar version of the random walk method presented in [7].

Fig. 4 shows the results of numerical simulation of the case with $\rho = 5$ considered in [25]. The total field $\Phi_1(r,\theta) \equiv Z_0 H_z(r,\theta)$ is plotted on the left diagram, while the field $\Phi_2(r,\theta)$ is plotted on the right diagram. We computed these fields along the arc $r = 4$ twice. Solid lines were computed by the code from [7] applied directly to the scalar problems from (2.5)–(2.7) with the diagonal matrices $A^\pm$ from (7.4). Bold dots show the results of computations by the probabilistic method of the present paper applied to the vector uncoupled problem (2.11)–(2.14) with the matrices $q^\pm$ from (7.5). It is obvious that our results obtained by the different methods agree with each other, as well as with the results from [25, Fig. 1] where they were obtained using the analytic Maliuzhinets method and by using the hybrid semi-analytic technique.

Finally, in the last series of numerical experiments we simulated diffraction in several cases which may not correspond to any existing material but are selected to test all the branches of the developed method. Fig. 5 shows the total wave field $\Phi_1(r,\theta)$ generated in the wedge $0 < \theta < 270^\circ$ by a plane incident wave (2.9) characterized by the amplitudes $p_h = 1$, $p_e = 0$ and by the angles $\theta_0 = 60^\circ$, $\beta = 60^\circ$. The impedances of both faces of the wedge are identical and correspond to the matrices $q^\pm$ from (2.14) which have one of the following values for six different cases

$$\begin{aligned} &a)\ q^\pm = \begin{pmatrix} 2.6 & 2.4 \\ 2.4 & 2.6 \end{pmatrix}, \quad b)\ q^\pm = \begin{pmatrix} 2.6 & 1 \\ -1 & 2.6 \end{pmatrix} \\ &c)\ q^\pm = \begin{pmatrix} 2.6 & \mathrm{i} \\ -\mathrm{i} & 2.6 \end{pmatrix}, \quad d)\ q^\pm = \begin{pmatrix} 2.6\mathrm{i} & 2.4 \\ 2.4 & 2.6\mathrm{i} \end{pmatrix} \\ &e)\ q^\pm = \begin{pmatrix} 2.6\mathrm{i} & \mathrm{i} \\ -\mathrm{i} & 2.6\mathrm{i} \end{pmatrix}, \quad f)\ q^\pm = \begin{pmatrix} 2.6\mathrm{i} & 1 \\ -1 & 2.6\mathrm{i} \end{pmatrix} \end{aligned} \tag{7.6}$$

obviously generalizing (7.5). All computations employed the averaging of 1000 random walks with the time increment $\Delta t = 0.025$. The infinite series in (5.11) was truncated after three consecutive new terms were smaller than 0.005. The covariance of statistical distributions did not exceed 0.5 near the boundaries, but were much lower in the middle of the wedge, which insures stable computations.

Comparing results in Fig. 5 with those in Fig. 4 we observe that even though θ_0, β and $q^\pm$ are different in the two figures, there is substantial similarity in the $\Phi_1(r,\theta)$ graphs. The primary difference is the height of the central peak in Fig. 5 the region $60^\circ < \theta < 80^\circ$.

VIII. Conclusion

The version of the random walk method developed in [3], [5]–[7] for scalar problems of diffraction is extended here to the three dimensional vector problem of electromagnetic diffraction of a plane skew incident wave by a wedge with different anisotropic impedance boundary conditions on its faces.

The obtained solution (5.11) is exact in the rigorous mathematical sense and it admits numerical implementation by simple algorithms with unlimited capability for parallel processing. As with analytic or asymptotic methods, the probabilistic solutions provided by the random walk method are local in the sense that they make it possible to compute functions of interest at individual points without computing them on dense meshes. Such solutions admit meaningful physical interpretations which do not contradict, but compliment, elementary models of wave

propagation employed by ray theory. All of these features together make the random walk method attractive for the analysis of wave propagation, and we hope that the present paper will stimulate its further development and practical use.

REFERENCES

[1] M. Abramowitz and I. A. Stegun, *Handbook of Mathematical Functions With Formulas, Graphs, and Mathematical Tables*, ser. Applied mathematics series. Washington, D.C.: U. S. Dept. of Commerce, National Bureau of Standards, 1972, vol. 55.

[2] J. M. L. Bernard, "Diffraction at skew incidence by an anisotropic impedance wedge in electromagnetism theory: a new class of canonical cases," *J. Phys. A, Mathematical and General*, vol. 31, pp. 595–613, 1998.

[3] B. V. Budaev and D. B. Bogy, "Random walk approach to wave propagation in wedges and cones," *J. Acoust. Soc. Amer.*, vol. 114, no. 4, pp. 1733–1741, 2003.

[4] ——, "Random walk approach to wave radiation in cylindrical and spherical domains," *Probabilistic Eng. Mechanics*, vol. 18, pp. 339–348, 2003.

[5] ——, "Diffraction by a plane sector," in *Proc. Royal Soc. A*, vol. 460, 2004, pp. 3529–3546.

[6] ——, "Diffraction of a plane wave by a sector with Dirichlet or Neumann boundary conditions," *IEEE Trans. Antennas Propag.*, vol. 53, no. 2, pp. 711–718, Feb. 2005.

[7] ——, "Two dimensional diffraction by a wedge with impedance boundary conditions," *IEEE Trans. Antennas Propag.*, vol. 53, no. 6, pp. 2073–2080, Jun. 2005.

[8] B. V. Budaev, *Diffraction by Wedges*, ser. Pitman research notes in mathematics series. New York: Longman Publishing, 1995, vol. 322.

[9] A. J. Chorin, "Accurate evaluation of Wiener integrals," *Math. Computations*, vol. 27, pp. 172–182, 1973.

[10] E. B. Dynkin and A. A. Yushkevich, *Markov Processes; Theorems and Problems*. New York: Plenum Press, 1969.

[11] E. B. Dynkin, "Markov processes," in *Die Grundlehren der Mathematischen Wissenschaften in Einzeldarstellungen*. Berlin, Germany: Springer-Verlag, 1965.

[12] P. E. Kloeden and E. Platen, *Numerical Solutions of Stochastic Differential Equations*. Berlin, Germany: Springer, 1992.

[13] W. Feller, *An Introduction to Probability Theory and its Applications*, ser. Wiley series in probability and mathematical statistics. New York: Wiley, 1967.

[14] M. Freidlin, "Functional Integration and Partial Differential Equations," in *The Annals of Mathematics Studies*. Princeton, NJ: Princeton Univ. Press, 1985.

[15] D. Friedman, *Brownian Motion and Diffusion*. San Francisco CA: Holden-Day, 1971.

[16] K. Ito and H. P. McKean Jr., *Diffusion Processes and Their Sample Paths*. Berlin, Germany: Springer-Verlag, 1965.

[17] Y. Y. Lobanov, "Deterministic computation of functional integrals," *Computational Phys. Commun* , vol. 99, pp. 59–72, 1996.

[18] M. A. Lyalinov and N. Y. Zhu, "Diffraction of a skewly incident plane wave by an anisotropic impedance wedge—a class of exactly solvable cases," *Wave Motion*, vol. 30, pp. 275–288, 1999.

[19] G. D. Maliuzhinets, "Radiation of sound by oscillating faces of an arbitrary wedge," *Acoust. J.*, vol. 1, no. 2, pp. 144–164, 1955.

[20] G. Manara, P. Nepa, G. Pelosi, and A. Vallecchi, "EM scattering from anisotropic impedance half-plane," *Electron. Lett.*, vol. 36, no. 6, pp. 505–506, 2000.

[21] ——, "Skew incidence diffraction by an anisotropic impedance half plane with a PEC face arbitrary oriented anisotropy axes," *Electron. Lett.*, vol. 36, no. 6, pp. 505–506, 2000.

[22] G. N. Milstein and M. V. Tretyakov, *Stochastic Numerics for Mathematical Physics*. Berlin, Germany: Springer, 2004.

[23] H. Niederreiter, "Quasi-Monte Carlo methods and pseudorandom numbers," *Bulletin American Math. Soc.*, vol. 84, pp. 957–1041, 1978.

[24] E. Novak, K. Ritter, and A. Steinbauer, "A multiscale method for the evaluation of Wiener integrals," *Approximation Theory X, v. 2, Computational Aspects*, pp. 251–258, 2002.

[25] A. V. Osipov, "A hybrid technique for the analysis of scattering by impedance wedges," in *Proc. URSI Int. Symp. Electromagn. Theory*, 2004, pp. 1140–1142.

[26] G. Pelosi, G. Manara, and P. Nepa, "Electromagnetic scattering by a wedge with anisotropic impedance faces," *IEEE Antennas Propag. Mag.*, vol. 40, no. 6, pp. 29–35, 1998.

[27] I. M. Ryzhik and I. S. Gradshtein, *Table of Integrals, Series, and Products*, 5th ed. San Diego, CA: Academic Press, 2000.

[28] B. Simon, "Functional integration and quantum physics," in *Pure and Applied Mathematics*. New York: Academic Press, 1979.

[29] I. Sloan and H. Wozniakowsky, "When are quasi-Monte Carlo algorithms efficient for high dimensional integrals," *J. Complexity*, vol. 14, pp. 1–33, 1998.

[30] A. Sommerfeld, "Mathematische theorie der diffraction," *Mathematische Annalen*, vol. 47, pp. 317–374, 1896.

[31] S. Tezuka, "Quasi-Monte Carlo method for financial applications," in *Proc. 4th Int. Congress Industrial and Applied Mathematics ICIAM'99*, Edinburg, 1999, pp. 234–245.

[32] N. Wiener, "Differential space," *J. Mathematical Phys.*, vol. 2, pp. 131–174, 1923.

[33] N. Y. Zhu and F. M. Landstorfer, "Numerical study of wave diffraction at scalar and tensor impedance wedges with the method of parabolic equation," in *Abstract Sommerfeld'96 Workshop: Modern Mathematical Methods in Diffraction Theory and its Applications in Engineering, Freudenstadt*, Black Forest, Germany, Sep.-Oct. 1996, pp. 43–44.

Bair V. Budaev received the M.S. (Diploma) and Ph.D. (Candidate of Sciences) degrees in applied mathematics and mechanics and the Doctor of Sciences degree from the Department of Mathematics and Mechanics, Leningrad State University, in 1976, 1979, and 1995, respectively.

In 1984, he joined the Staff of the St. Petersburg Branch of the Steklov Mathematical Institute. Since 1995, he has continued his research at the University of California, Berkeley.

David B. Bogy received the B.S. degree in geology and in mechanical engineering and the M.S. degree in mechanical engineering from Rice University, Houston, TX, in 1959 and 1961, respectively, and the Ph.D. degree in applied mathematics from Brown University, Providence, RI, in 1966.

He spent a year as a Postdoctoral Fellow at the California Institute of Technology, Pasadena. In 1967, he joined the Faculty of the University of California at Berkeley. From 1991 to 1999, he was Chairman of the Department of Mechanical Engineering, University of California at Berkeley.

Prof. Bogy is a Member of the National Academy of Engineering and serves on the U.S. National Committee on Theoretical and Applied Mechanics. He was Chair of the Executive Committees of the Applied Mechanics and the Tribology Divisions of the American Society of Mechanical Engineers.